

Original Article

Dlx5 and Msx2 regulate mouse anterior neural tube closure through ephrinA5-EphA7

Jangwoo Lee,^{1,3*} Amy Corcoran,² Manjong Han,¹ David M. Gardiner³ and Ken Muneoka¹

¹Department of Cell and Molecular Biology, School of Science and Engineering, Tulane University, New Orleans, Louisiana, 70115, ²University of Illinois at Chicago College of Medicine, Chicago, Illinois, 60612, and ³Department of Developmental and Cell Biology, School of Biological Sciences, University of California at Irvine, Irvine, California, 92697, USA

Homeodomain-containing transcription factors Dlx5 and Msx2 are able to form a heterodimer, and together can regulate embryonic development including skeletogenesis. Dlx5 functions as a transcriptional activator and Msx2 a transcriptional repressor, and they share common target genes. During mouse digit development, the expression domains of *Dlx5* and *Msx2* overlap at the distal region of the developing terminal phalange, although digit formation and regeneration are not altered in the *Dlx5* and *Msx2* null mutant embryos. Interestingly, we observed a high rate of defects in neural tube formation in *Dlx5* and *Msx2* double null mutants. In the absence of both *Dlx5* and *Msx2*, a high occurrence of exencephaly and severe defects in craniofacial morphology are observed. Additionally, *Dlx5* and *Msx2* expression domain analysis showed overlap of the genes at the apex of the neural folds just prior to neural fold fusion. The expression patterns of *ephrinA5* and two isoforms of *EphA7* were tested as downstream targets of Dlx5 and Msx2. Results show that *EphrinA5* and the truncated isoform of *EphA7* are regulated by Dlx5 and Msx2 together, although the full length isoform of *EphA7* expression is not altered. Overall, these data show that Dlx5 and Msx2 play a critical role in controlling cranial neural tube morphogenesis by regulating cell adhesion via the ephrinA5 and EphA7 pathway.

Key words: Dlx5, EphA7, ephrinA5, Msx2, neural tube formation.

Introduction

Neurulation is a fundamental process that establishes the neural system during embryonic development. The neural tube is the major structure that forms during neurulation, and represents the anlagen of the brain and spinal cord. The neural tube is formed by the progressive fusion of the neural folds, which are elevated tissue structures along the lateral edges of the neural plate at the dorsal midline of the embryo. Approximately 80 genes are involved in a mammalian neurulation, and neural tube defects (NTDs) result with disruption of any of these genes (Copp *et al.* 2003). Anencephaly is one such NTD that is caused by a neural patterning defect and results from disrupted

tube closure in the cranial region of the embryo. Anencephaly is the resulting phenotype when exencephalic brain tissue gradually degenerates due to the exposure to amniotic fluid (Timor-Tritsch *et al.* 1996). In humans, the occurrence rate of the NTDs is approximately 1 out of 1000–2000 births in the United States (Copp *et al.* 2003).

Among the genes that are involved in neurulation, *Dlx* (distal-less homeobox) and *Msx* (msh-like homeobox) family genes have been reported for their roles in craniofacial embryogenesis, including anterior neural tube formation. Both the *Dlx* and *Msx* gene families encode for homeodomain-containing transcription factors. In mammals there are six members of the *Dlx* family (*Dlx1–6*) and three members of the *Msx* family (*Msx1–3*) (Depew *et al.* 2005; Ramos & Robert, 2005). The *Dlx* gene family has been implicated in embryonic development including brain, branchial arches, jaws and limb development (Depew *et al.* 2005). In a *Dlx5* gene null mutant study, it was demonstrated that approximately 24% of mutant embryos showed an exencephaly phenotype at E13.5 (Depew *et al.* 1999) and this phenotype is more severe in the *Dlx5/6* dou-

*Author to whom all correspondence should be addressed.

Email: jangwool@uci.edu

Received 13 August 2012; revised 9 January 2013; accepted 10 January 2013.

© 2013 The Authors

Development, Growth & Differentiation © 2013 Japanese Society of Developmental Biologists

ble mutant, suggesting that these genes play a redundant role in anterior neural tube patterning (Robledo *et al.* 2002). In the case of the *Msx* gene family, all three *Msx* genes are expressed during neurulation (Shimeld *et al.* 1996; Ramos & Robert 2005), and based on knockout studies, it has been demonstrated that *Msx1* and *Msx2* regulate craniofacial patterning processes (Satokata & Maas, 1994; Satokata *et al.* 2000; Bach *et al.* 2003). While neither *Msx1* nor *Msx2* single gene mutation cause anterior neural tube closure defect, the majority of *Msx1/2* double null mutant embryos fail to close the anterior neural pore and exhibit severe craniofacial abnormalities including exencephaly (Han *et al.* 2007). These studies suggest that both the *Dlx* and *Msx* gene families are critical for proper neural tube formation, and in both cases there is evidence that their family members serve redundant roles.

Previous studies have demonstrated that *Msx* and *Dlx* homeoprotein families form homo- and heterodimeric complexes and suggests that protein–protein interactions can be an essential molecular event in particular regulation of gene expressions (Zhang *et al.* 1997). *Dlx5* is known to function as a transcriptional activator and *Msx2* as a transcriptional repressor, and these genes directly regulate a number of target genes including *Runx2* (Shirakabe *et al.* 2001; Kim *et al.* 2004), *Osteocalcin* (Newberry *et al.* 1998), and *BMP2* induced alkaline phosphatase (Kim *et al.* 2004).

Membrane-bound GPI (glycosyl phosphatidylinositol)-anchored ligands ephrins and its receptor Ephs play key roles in diverse biological processes. Receptor Ephs are a subgroup of tyrosine protein kinase receptor family (Campbell & Robbins 2008; Klein 2009). The Eph receptors and their ephrins ligands are divided into A- and B-subclass based on their molecular structure and binding affinities (Frisen *et al.* 1999). To date, five type-A ephrins (ephrinA1–A5), three type-B ephrins (ephrinB1–B3), nine type-A Ephs (EphA1–A8 and A10), and five type-B Ephs (EphB1–B4 and EphB6) have been identified in mammals (Klein 2009). It has been described that members of A-subclass, ephrinA5 and EphA7 function in the neural fold fusion through cellular adhesion/repulsion. A subpopulation of *ephrinA5* (17%) mutant mice, as well as *EphA7* (24%) mutant, exhibit cranial neural tube malformation due to a neural tube fusion defect (Frisen *et al.* 1999). The receptor EphA7 has three splice variants; one full length form (EphA7-FL) and two truncated forms both of which lack a cytoplasmic tyrosine kinase domain (EphA7-T1, EphA7-T2, Ciossek *et al.* 1995; Valenzuela *et al.* 1995; Frisen *et al.* 1999). When ephrinA5 ligand on one cell is bound to EphA7-FL homo-dimer on an adjacent cell, these two cells repulse each other. However, if ephrinA5 binds to EphA7-FL/EphA7-T1 or T2 heterodi-

mer, the two cells will adhere together. This report suggests that regulation of cell adhesion and repulsion processes by ephrinA5/EphA7 plays a critical role in controlling cranial neural tube formation (Frisen *et al.* 1999).

To date, although many studies unveiled the molecular mechanisms of cranial neural tube patterning from a genetic-based approach, many aspects of the molecular networks of cranial neural tube patterning remain unknown. In this report, we demonstrated that *Dlx5/Msx2* double mutants display an increased rate of malformation in cranial neural tube formation as compared to *Dlx5* or *Msx2* single mutants. Our studies show that the frequency of exencephaly increases incrementally in a *Dlx5* mutant background with decreasing *Msx2* gene dose. In addition, *ephrin-A5* and *EphA7-T1* expression, but not *EphA7-FL*, were downregulated in *Dlx5/Msx2* double mutant embryos at the dorsal region of neural tube in association with the failure of neural fold fusion. Our report provides a novel molecular mechanism in which *Dlx5* and *Msx2* function reciprocally through the regulation of *ephrin-A5/EphA7* expression in cranial neural tube closure.

Materials and methods

Wildtype and Dlx5, Mx2 mutant mice

Wildtype mouse embryos used in this study were either outbred CD#1 strain supplied by Charles River Laboratories or wildtype embryos from the breeding of *Dlx5* and *Msx2* mutant mice. Homozygous *Dlx5* or *Msx2* mutant embryos were obtained by mating of heterozygotes carrying a targeted deletion of either the *Dlx5* gene (Depew *et al.* 1999) or the *Msx2* gene (Satokata *et al.* 2000). *Dlx5/Msx2* double mutant embryos were obtained by double heterozygotes mating. Embryos were collected at embryonic day (E) 9.5 and their genotype was verified by polymerase chain reaction (PCR) with genotype specific PCR primers. Procedures for the care and use of mice for this study were compliant with standard operating procedures (SOPs) approved by the Institutional Animal Care & Use Committee (IACUC) of Tulane University Health Science Center.

Fetal mouse digit amputation

To study regeneration *in vivo*, fetal mouse digit tips were amputated at E14.5. Timed-pregnant mice, which carry E14.5 embryos were anesthetized with sodium pentobarbital (60 µg/g body weight), fentanyl (1.6 µg/animal), and droperidol (80 µg/animal). The pregnant mouse abdomen was opened with a mid-

ventral incision, and fetuses were exposed by incision of the anti-placental uterine wall. Access to the hindlimb was gained through an incision in the extraembryonic membranes and the hindlimb was teased out with a blunt probe. The three central hindlimb digits, digits 2, 3, and 4, were amputated at a distal level, approximately 75 mm from the digit tip. The uterus with attached fetuses was re-positioned within the abdominal cavity, and the abdominal wall of female mouse was closed. Operated fetuses were allowed to develop for 4 days *ex utero* (Muneoka *et al.* 1986), after which the hindlimbs were collected for analysis of the digits.

Whole mount skeletal staining

Differential whole mount bone staining of mouse embryos was performed according to the following process. Embryos were isolated at E18.5 and fixed with 95% ethanol (EtOH) overnight. Embryos were then skinned manually, delipidated in acetone, and stained with Alcian Blue 8XG/Alizarin Red S in 5% acetic acid, 95% EtOH. Stained embryos were treated in 1% KOH and cleared by glycerol.

In situ hybridization

Digoxigenin-labeled antisense RNA probes for *Dlx5*, *Msx2*, *EphrinA5*, *EphA7-FL*, and *EphA7-T1* were used to perform *in situ* hybridization. *EphrinA5*, *EphA7-FL*, and *EphA7-T1* containing DNA plasmids were kindly provided by Dr Jonas Frisén. Embryos were collected at E 9.5 and fixed in 4% paraformaldehyde at 4°C overnight. Fixed mouse embryos were dehydrated with an ascending series of ethanol (25%, 50%, 75% and 100%), infiltrated in xylene, and embedded in paraffin. Paraffin sections were cut at 5 µm thickness. *In situ* hybridization was performed according to previous method (Han *et al.*, 2003).

Results

Dlx5 and *Msx2* in mouse fetal digit regeneration

The transcriptional repressor *Msx1* and cell signaling molecule *Bmp4* are co-expressed at the apex of the forming fetal mouse digit and both have been implicated in the control of digit tip regeneration (Han *et al.* 2003). DLX and MSX proteins can form heterodimers that can regulate gene transcriptions (Zhang *et al.* 1997). Particularly, the DLX5 and MSX2 have been shown to form a heterodimeric complex that regulates differentiation during skeletogenesis (Newberry *et al.* 1998). To study the role of *Dlx5* and *Msx2* in digit

regeneration we began by analyzing the expression of *Dlx5* and *Msx2* on mouse digit at E14.5. Expression of *Dlx5* was detected in ectoderm and mesenchymal tissue between the epidermis and condensed cartilage of digit (Fig. 1A). The *Msx2* expression pattern is similar to the expression of *Dlx5* at the digit tip, but extended proximally (Fig. 1B). Since *Msx2* and *Dlx5* are co-expressed at the apex of the forming digit, we were interested in whether these two genes were involved in the control of fetal digit regeneration. The *Msx2* mutant digit had previously been tested and was found to regenerate normally, thus suggesting that *Msx2* was not required for digit tip regeneration (Han *et al.* 2003). Here we tested the regenerative capacity of *Dlx5* mutant digits at E14.5, and as well, we re-tested the *Msx2* mutant. We found that the *Dlx5* and *Msx2* mutant digits possessed a regenerative capacity similar to wildtype digits, thus indicating that neither gene was required for fetal digit tip regeneration (Table 1). To test the role of both *Dlx5* and *Msx2* in fetal digit regeneration, we generated *Dlx5*^{-/-}; *Msx2*^{-/-} double mutant embryos. E14.5 digits from this double mutant were tested for regenerative ability and their regenerative response was undistinguishable from wildtype control digits (Table 1). These studies demonstrate that despite their co-expression at the apex of the forming digit and their known interactions in regulating skeletogenesis, *Dlx5* and *Msx2* do not appear to play a functional role in fetal digit tip regeneration.

Exencephaly phenotype in *Dlx5* and *Msx2* double mutant mouse embryo

During our studies on the role of *Dlx5* and *Msx2* in fetal digit tip regeneration, we noted that the most dramatic phenotype associated with the double mutant embryos was that many embryos displayed exencephaly. It has

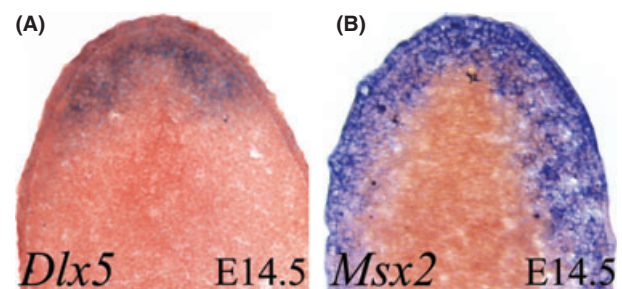


Fig. 1. Expression domains of *Dlx5* and *Msx2* overlap in fetal digit tip. (A–B) Expression of *Dlx5* (A) and *Msx2* (B) are detected in ectoderm and mesenchymal tissue of the E14.5 fetal mouse digit tip. The expression domain of *Dlx5* is restricted to the distal region of the digit (A), but *Msx2* expression domain is extended more proximally (B).

Table 1. Regeneration response of fetal digit tips

	Genotype					
	WT	<i>Dlx5</i> ^{+/-}	<i>Dlx5</i> ^{-/-}	<i>Msx2</i> ^{-/-}	<i>Dlx5</i> ^{+/-} ; <i>Msx2</i> ^{-/-}	<i>Dlx5</i> ^{-/-} ; <i>Msx2</i> ^{-/-}
Number of regenerated digit	25/27 (92.6%)	46/48 (95.8%)	17/18 (94.4%)	6/6 (100%)	27/30 (90.0%)	30/30 (100%)

WT, wildtype.

been already reported that 12% or 28% of *Dlx5* null mutant embryos displayed an exencephalic phenotype (Acampora *et al.* 1999; Depew *et al.* 1999), but that exencephaly was not noted in *Msx2* null embryos (Satokata *et al.* 2000). To characterize the exencephalic phenotype among the different genotypes of embryos developing from a double heterozygote cross, we collected embryos from stages ranging from E9.5 to E18.5 to establish the frequency of exencephaly. In this analysis we obtained and scored embryos with multiple genotypes, including wildtype, *Dlx5*^{-/-}, *Msx2*^{-/-}, *Dlx5*^{+/-};*Msx2*^{+/-}, *Dlx5*^{+/-};*Msx2*^{-/-}, *Dlx5*^{-/-};*Msx2*^{+/-}, and *Dlx5*^{-/-};*Msx2*^{-/-} (Table 2). Similar to previous studies, we found that 19% of *Dlx5* null mutant embryos displayed exencephaly while *Msx2* null mutants had no exencephalic embryos. *Dlx5* heterozygote embryos display no exencephaly (Acampora *et al.* 1999; Depew *et al.* 1999); however, if the embryos lack either one or both copies of *Msx2* they display a low level of exencephaly (*Dlx5*^{+/-};*Msx2*^{+/-}: 7%; *Dlx5*^{+/-};*Msx2*^{-/-}: 9%). Interestingly, in a *Dlx5* mutant background, the frequency of exencephaly increased to 39% when one copy of *Msx2* is absent, and when both copies are absent the exencephalic frequency jumps to 73%. These studies clearly show that the exencephaly phenotype associated with the *Dlx5* mutant is influenced by *Msx2* in a synergistic manner.

Since *Dlx5* and *Msx2* are both transcriptional regulators and are known to interact during skeletogenesis, we next analyzed skull formation of neonates in whole mount skeletal preparations of *Msx2* mutants, and of *Dlx5*^{-/-} and *Dlx5*^{+/-};*Msx2*^{-/-} mutants displaying

exencephaly at E18.5. Ossifying frontal, parietal, interparietal, and supraoccipital bones are shown in the calvarium of wildtype embryos at E18.5 (Fig. 2A,B). Skull morphology of the *Msx2* null mutant shows that skull size was slightly reduced in comparison to wildtype controls, and that ossification of interparietal and supraoccipital bones is delayed (arrows in Fig. 2E,F). On the other hand the frontal and parietal bones are not affected in the *Msx2* mutant. The size of the calvarium of the *Dlx5*^{-/-} exencephaly phenotype is grossly reduced, and all five fontanelle bones as well as the supraoccipital bone do not form (Fig. 2C,D). Similarly, in the *Dlx5* and *Msx2* double null mutant embryo the calvarium displays an identical morphology to the *Dlx5* mutant (Fig. 2G,H). We also examined the whole mount skull sample of non-exencephaly embryos of *Dlx5*^{-/-};*Msx2*^{-/-} mutants. Although the epidermis of the cranium is intact, frontal, parietal and interparietal bones were only partially developed, and the supraoccipital bones were missing (Fig. 2I,J). While the cranial phenotypes vary depending on genotype, gross morphologies of embryos are not significantly altered from wildtype (Fig. S1). These data show that the primary effect of removing copies of the *Msx2* gene on the *Dlx5* mutant is associated with the frequency of exencephaly and not the severity of phenotype. This finding, combined with evidence that the expression domains of *Dlx5* and *Msx2* do not overlap during the embryogenesis of the skull (Kim *et al.* 1998; Holleville *et al.* 2003) suggests that the exencephalic defect caused by the double mutation is linked to developmental events that precede skeletogenesis.

Table 2. Exencephalic phenotype ratio in different mouse genotypes

Stage	Genotype					
	<i>Dlx5</i> ^{-/-}	<i>Msx2</i> ^{-/-}	<i>Dlx5</i> ^{+/-} ; <i>Msx2</i> ^{+/-}	<i>Dlx5</i> ^{+/-} ; <i>Msx2</i> ^{-/-}	<i>Dlx5</i> ^{-/-} ; <i>Msx2</i> ^{+/-}	<i>Dlx5</i> ^{-/-} ; <i>Msx2</i> ^{-/-}
E9.5	1/6	0/13	3/20	1/9	4/11	8/10
E10.5	1/2	0/5	0/17	0/7	3/8	2/5
E11.5	0/2	0/2	2/12	2/5	3/7	1/2
E12.5	0/2	0/5	0/15	0/7	3/5	1/1
E14.5	N/A	0/12	0/8	2/22	1/5	13/18
E18.5	1/4	0/1	0/3	0/5	N/A	5/5
Total	3/16 (18.8%)	0/38 (0%)	5/75 (6.7%)	5/55 (9.1%)	14/36 (38.9%)	30/41 (73.2%)

N/A, data not available.

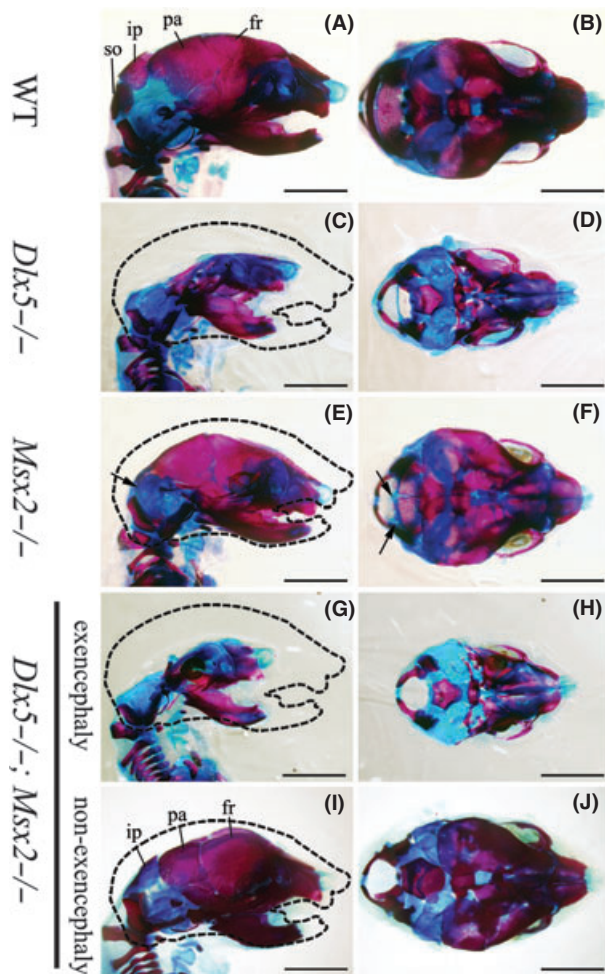


Fig. 2. Gross skull morphology of wildtype (WT), *Dlx5*^{-/-}, *Msx2*^{-/-}, and *Dlx5*;*Msx2*^{-/-} mutant mouse embryos. (A–J) At E18.5, differential skeletal staining images of embryo calvaria with lateral view (A, C, E, G, I) and dorsal view (B, D, F, H, J). (A, B) Wildtype. (C, D) *Dlx5*^{-/-}. Fontanelle and supraoccipital bones are missing. (E, F) *Msx2*^{-/-}. Ossification of interparietal and supraoccipital bones are delayed (arrows). (G, H) Exencephaly embryo of *Dlx5*^{-/-};*Msx2*^{-/-}. The skull morphology is similar to *Dlx5* single mutant. (I, J) Non-exencephaly embryo of *Dlx5*^{-/-};*Msx2*^{-/-}. The frontal, parietal and interparietal bones are only partially developed, and the supraoccipital bone is missing. Black dot lines indicate the outline of the wildtype embryo skull. fr, frontal bone; ip, interparietal bone; pa, parietal bone; so, supraoccipital bone. Scale bars: 3 mm.

Dlx5 and *Msx2* expression patterns during cranial neural tube formation

The cause of the exencephaly phenotype is generally linked to a failure of the anterior neural tube to close properly during neurulation early in embryogenesis (Copp *et al.* 2003). Double mutant embryos analyzed for exencephaly confirm that the phenotype is present in the early embryo (Table 2), and is associated with

the failure of the anterior neural tube to close. To investigate the role of *Dlx5* and *Msx2* in neural tube closure we first carried out a detailed analysis of gene expression during neurulation. The neurulation process can be divided into four stages: (i) formation of neural plate; (ii) folding of the neural plate to form the neural groove; (iii) elevation of the neural folds; and (iv) closure of the neural folds to form the neural tube (Gilbert 2003). The cranial region of the mouse embryo undergoes its incipient neural groove stage at E8.5. At this time point, *Dlx5* transcripts were not detected anywhere in the neural folds (Fig. 3A), whereas *Msx2* expression was detected at the edges of the neural folds (black arrowheads, Fig. 3D). At E9.5, neural tube formation is completed in the cranial region of the embryo and both the neural fold elevation stage and neural tube stage can be observed in the same embryo analyzed at different cranial-caudal levels. *Dlx5* is transiently expressed at the apex of the neural folds (black arrowheads, Fig. 3B); however, after closure of the neural tube *Dlx5* expression is downregulated and is no longer detected in the neural tube (Fig. 3C). During this stage *Msx2* transcripts are detected in the apex of neural folds in a region that overlaps the expression domain of *Dlx5* (Fig. 3E). After closure of the neural tube *Msx2* remains expressed at the point of fusion along the dorsal midline (black arrowheads, Fig. 3E,F). Summarizing, *Msx2* is expressed in the apex of the neural folds and at the dorsal midline of the neural tube during and after fusion to close the anterior neural tube, whereas *Dlx5* is transiently upregulated in the apex of the neural folds immediately prior to neural fold fusion and downregulated after fusion (Fig. 3G). In terms of expression domain, *Dlx5* and *Msx2* expression sites overlap in the apex of the neural folds just prior to fusion (Fig. 3B,E).

EphrinA5 and *EphA7* are regulated by *Dlx5* and *Msx2* together

The developmental expression of *Dlx5* and *Msx2* suggests that the exencephaly phenotype associated with the double mutation may be linked to a synergistic interaction between these two genes during a transient period when they are both expressed at the apex of the neural folds during neural fold fusion. Since both *Dlx5* and *Msx2* are transcriptional regulators that must regulate morphogenetic events by affecting the expression of structural genes, we explored potential downstream target genes that might be linked to the exencephaly phenotype. In a previous report, it has been demonstrated that ephrinA5 and its receptor *EphA7* participate in cranial neural tube morphogenesis via cell attraction and cell repulsion, and that

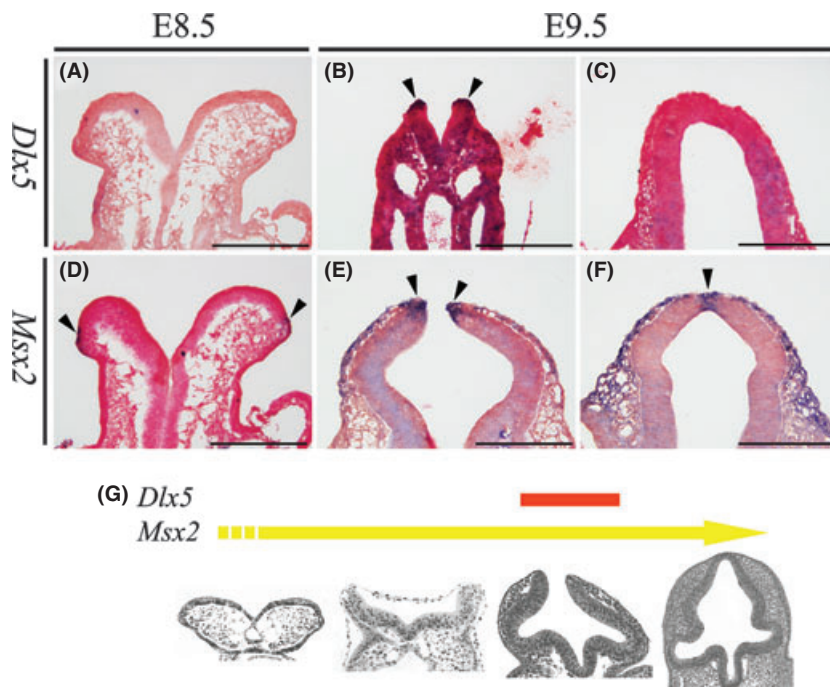


Fig. 3. Expression patterns of *Dlx5* and *Msx2* during cranial neural tube formation. (A–C) Expression of *Dlx5* at E8.5 (A) and E9.5 (B, C). *Dlx5* transcripts are detected transiently prior to neural tube closure at E9.5 (arrowheads in b), and the transcripts are no longer observed after neural tube closure (c). (D–F) Expression of *Msx2* at E8.5 (D) and E9.5 (E, F). Expression of *Msx2* is detected before neural tube closure (arrowhead in D), and its expression is detected continuously at the point of fusion (arrowheads in E and F). (G) Schematic diagram of temporal expression pattern of *Dlx5* (Orange line) and *Msx2* (yellow line) during cranial neural folds fusion. The cranial neural tube formation images are modified from the e-Mouse Atlas (www.emouseatlas.org). Scale bars: 100 μ m.

embryos that possess a defect in this signaling pathway can display exencephaly (Holmberg *et al.* 2000). To explore whether *Dlx5* and *Msx2* have a regulatory role on the expression of *ephrinA5*, *EphA7-FL*, and *EphA7-T1*, we performed gene expression pattern analysis of *ephrinA5*, *EphA7-FL*, and *EphA7-T1* on WT, *Dlx5*^{-/-}, *Msx2*^{-/-}, and *Dlx5*^{-/-};*Msx2*^{-/-} mouse embryos at E9.5 (two embryos were used in each genotype for the gene expression pattern analysis). In wildtype embryos, the expression domain of *ephrinA5* and *EphA7-FL* are almost identical to each other in that expression is restricted to the outer layer of the neural tube (Fig. 4A,E). The expression domain of *EphA7-T1* is in the dorsal two-thirds of the neural tube (Fig. 4I, the ventral margin of *EphA7-T1* expression domain indicated by arrows), and the domain is broader than *ephrinA5* and *EphA7-FL*. In *Dlx5* null mutant embryos, expression of *ephrinA5* and *EphA7-FL* appeared similar to wildtype embryos (Fig. 4B,F). However, *EphA7-T1* expression domain was expanded to the ventral region of the neural tube in *Dlx5*^{-/-} mutants, although the intensity of expression did not appear to be significantly changed (Fig. 4J). In *Msx2* null mutant embryos, expression of *EphA7-FL* was not changed (Fig. 4G), whereas *ephrinA5* expression was slightly decreased (Fig. 4C). The expression domain of *EphA7-T1* in *Msx2* mutant was expanded to the ventral region, but the expression level was not altered (Fig. 4K). In *Dlx5* and *Msx2* double null mutant embryos displaying exencephaly the expression of *ephrinA5* was decreased all over the neural tissue,

particularly in the region of *Dlx5*/*Msx2* co-expression at the apex of the neural folds (Fig. 4D). *EphA7-FL* expression was not modified in the apex of neural folds in *Dlx5*^{-/-};*Msx2*^{-/-} embryos (Fig. 4H), whereas *EphA7-T1* transcripts were largely absent throughout the neural tissue including the apex of the neural folds (Fig. 4D,L). These results show that the expression of the ligand, *ephrinA5*, and one of its receptors, *EphA7-T1*, is regulated by the combined activity of *Dlx5* and *Msx2* during anterior neural tube closure.

Discussion

In the mouse, neural tube closure initiates at three different points along the cranial-caudal axis. The primary initiation point (closure 1) is located at the hindbrain/cervical boundary, and closure then proceeds in both cranial and caudal directions. The second neural tube closure (closure 2) initiation point is located at the forebrain/midbrain boundary. The last neural tube closure (closure 3) initiation point is located at the extreme rostral end of the embryo, and closure proceeds in the caudal direction (Copp *et al.* 2003). In this study we focused on the role of *Dlx5* and *Msx2* in cranial neural tube closure (closure 2) and found that *Dlx5* and *Msx2* are co-expressed at the apex of the neural folds during neural tube formation. Using *Dlx5* and *Msx2* genetically disrupted mice, we confirm a low frequency of exencephaly in the *Dlx5* mutant (Depew *et al.* 1999), and found that the frequency of exencephaly

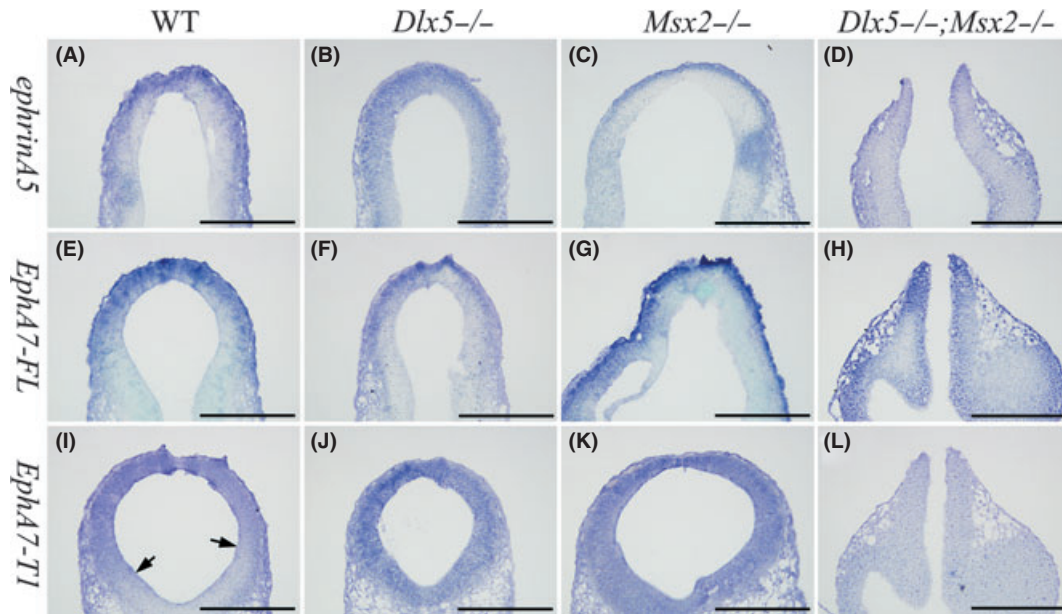


Fig. 4. Expression pattern of *ephrinA5*, *EphA7-FL*, and *EphA7-T1* in WT, *Dlx5*^{-/-}, *Msx2*^{-/-}, and *Dlx5*^{-/-};*Msx2*^{-/-} mice embryos at E9.5. (A–D) Expression of *ephrinA5* in wildtype (A), *Dlx5*^{-/-} (B), *Msx2*^{-/-} (C), and *Dlx5*^{-/-};*Msx2*^{-/-} (D). Transcripts of *ephrinA5* are detected outer layer of the neural tube. This expression is not altered in *Dlx5*, or slightly decreased in *Msx2* mutant. In contrast, the double mutant embryo shows significantly decreased expression of *ephrinA5*. (E–H) Expression of *EphA7-FL* in wildtype (E), *Dlx5*^{-/-} (F), *Msx2*^{-/-} (G), and *Dlx5*^{-/-};*Msx2*^{-/-} (H). Expression pattern of *EphA7-FL* is not modified in *Dlx5*, *Msx2*, or the double mutant. (I–L) Expression of *EphA7-T1* in wildtype (I), *Dlx5*^{-/-} (J), *Msx2*^{-/-} (K), and *Dlx5*^{-/-};*Msx2*^{-/-} (L). Expression domain of *EphA7-T1* in the neural tube is expanded toward the ventral side in *Dlx5* and *Msx2* single mutant embryo. In *Dlx5*/*Msx2* double mutant, *EphA7-T1* expression is significantly decreased. Scale bars: 100 μ m.

becomes more severe with the sequential removal of *Msx2* alleles. Since *Dlx5* is a known transcriptional activator and *Msx2* is a transcriptional repressor known to heterodimerize and/or compete with *Dlx5* for DNA binding to antagonize *Dlx5* activity (Zhang *et al.* 1997), the observed genetic interaction between *Dlx5* and *Msx2* in the double mutant poses a bit of a conundrum that requires further investigation. A similar synergistic interaction between *Dlx5* and *Msx1* has been reported in association with frontal bone development (Chung *et al.* 2010). Based on these results the simple interpretation that the loss of a transcriptional repressor would phenotypically cancel the loss of a transcriptional activator seems unlikely.

Functional redundancy among members of the *Dlx* or *Msx* families has been previously demonstrated (Robledo *et al.* 2002; Lallemand *et al.* 2005). Within the *Dlx* family, *Dlx5* and *Dlx6* are very similar in their expression pattern, homology of the amino acid sequences (Merlo *et al.* 2000; Zerucha *et al.* 2000), and they have redundant function in limb development and cranial neural tube formation (Robledo *et al.* 2002). Similarly, in the *Msx* family, redundancy has also been demonstrated in the regulatory function of *Msx1* and *Msx2* in limb development and cranial neural tube formation (Lallemand *et al.* 2005; Han *et al.*

2007). Therefore, the functional redundancy among the *Dlx* transcriptional activators and the *Msx* transcriptional repressors can account for the dose-related effects of *Msx2* in a *Dlx5* mutant background. Thus, the functional redundancy within *Dlx* and *Msx* family members, the established functional antagonism between *Dlx5* and *Msx2*, and the co-expression of *Dlx5* and *Msx2* at the tips of the neural fold prior to fusion suggest that the interaction between *Dlx* and *Msx* proteins play a primary regulatory role in controlling neural tube closure. This conclusion is further supported by gain of function studies in which *Msx2* overexpression also results in a low frequency of exencephalic embryos (Winograd *et al.* 1997).

Our *Dlx5*/*Msx2* mutant studies identified that the expression of the *ephrinA5* gene and transcripts of the truncated form of its receptor gene, *EphA7-T1*, are downregulated during neural tube formation. These data provide evidence of molecular networking between *Dlx5*/*Msx2* and *ephrinA5*/*EphA7* in cranial neural tube morphogenesis (Fig. 5A,B); however, the detailed molecular mechanisms of this network are not clear at this time. The expression domains of *Dlx5* and *Msx2* are restricted to the very tip of the neural folds, whereas transcripts of *ephrinA5*, *EphA7-FL*, and *EphA7-T1* are detected broadly in the dorsal side of neural folds and

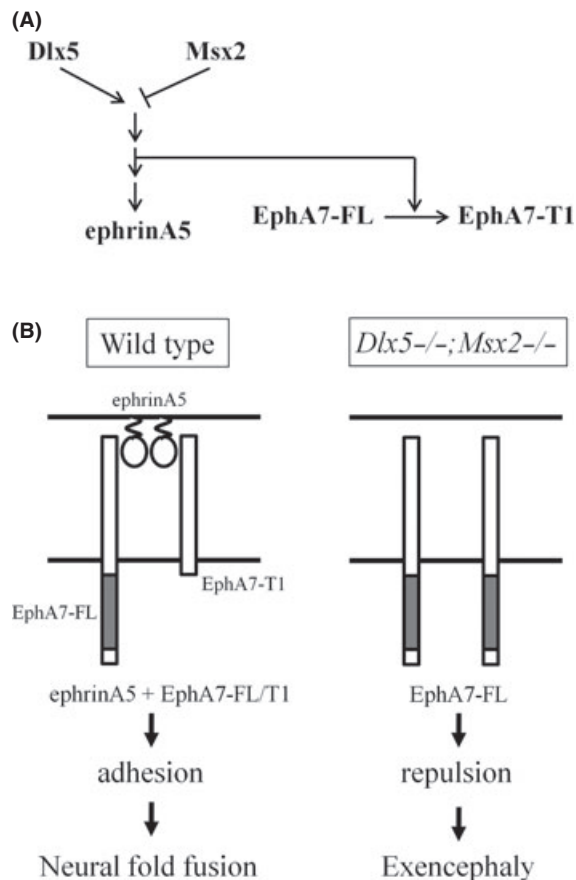


Fig. 5. Dlx5/Msx2 regulates ephrinA5/EphA7-T1 during cranial neural fold fusion. (A) This model demonstrates that Dlx5/Msx2 regulates expression of *ephrinA5*, and pre-mRNA alternative splicing process of *EphA7* transcripts to the truncated isoform (EphA7-T1). (B) Schematic diagram demonstrates a model that ephrinA5/EphA7 combination in wildtype and *Dlx5* and *Msx2* double mutant results either in cell adhesion or cell repulsion.

the neural tube. These non-overlapping expression domains suggest an indirect regulatory interaction possibly involves downstream signaling between cells of the neural fold. However, it is clear that the *ephrinA5* gene is a downstream target in this pathway, whereas the *EphA7* gene is not. It is also important to note that the frequency of neural tube closure defect in the *Dlx5*/*Msx2* double mutants is four times greater than the *ephrinA5* null mouse, thus indicating additional downstream targets modulating neural tube closure.

Transcripts for the *EphA7* gene encode for a full-length receptor (EphA7-FL), and two tyrosine kinase domain truncated isoforms, EphA7-T1 and EphA7-T2, which are the products of alternative splicing (Ciossek *et al.* 1995; Valenzuela *et al.* 1995). Since Dlx5/Msx2 regulates expression of a truncated isoform of *EphA7*, but not the full length isoform, Dlx5/Msx2 must regulate the mechanism by which *EphA7* RNA is differentially

spliced. To date, there is no evidence for regulation of pre-mRNA alternative splicing by Dlx or Msx transcription factors. However, modulation of the 5'-splice site by the transcription factor c-Myb has been reported (Orvain *et al.* 2008). Further investigations into this novel molecular network in which Dlx5/Msx2 regulates neural fold morphogenesis by controlling differential cell adhesion via ephrinA5/EphA7 interactions is necessary for our understanding of cranial neural fold fusion.

With respect to the developing digit we find that despite overlapping expression domains at the digit tip, an interaction between Dlx5 and Msx2 is not functionally linked to either digit tip formation or regeneration. Since other Dlx and Msx family members are co-expressed in similar domains (Robledo *et al.* 2002; Han *et al.* 2003) it is reasonable to conclude that functional redundancy may be masking any phenotypic defect. However, the discovery of a Dlx5/Msx2 link to the control of *ephrinA5*/*EphA7* activity during neural tube closure is suggestive that this signaling network may be conserved during digit formation and regeneration. The role of ephrin/Eph signaling in mammalian digit regeneration has not been explored in detail; however, differential cell adhesion is known to play a critical role both during limb development and limb regeneration (see Wada 2011) making further exploration of this molecular network primed for future studies.

Acknowledgments

We thank the Muneoka lab for discussions and Dr Robert Kosher for kindly providing the *Dlx5* mutant. Also, we thank Dr Jonas Frisén for kindly providing the *EphrinA5*, *EphA7-FL*, and *EphA7-T1* containing DNA plasmids. Research funded by P01HD022610 from the NIH, W911NF-06-1-0161 from DARPA, W911NF-09-1-0305 from the US Army Research Center, and the John L. and Mary Wright Ebaugh endowment fund at Tulane University.

References

- Acampora, D., Merlo, G. R., Paleari, L., Zerega, B., Postiglione, M. P., Mantero, S., Bober, E., Barbieri, O., Simeone, A. & Levi, G. 1999. Craniofacial, vestibular and bone defects in mice lacking the distal-less-related gene *Dlx5*. *Development* **126**, 3795–3809.
- Bach, A., Lallemand, Y., Nicola, M. A., Ramos, C., Mathis, L., Maufrais, M. & Robert, B. 2003. *Msx1* is required for dorsal diencephalon patterning. *Development* **130**, 4025–4036.
- Campbell, T. N. & Robbins, S. M. 2008. The eph receptor/ephrin system: an emerging player in the invasion game. *Curr. Issues Mol. Biol.* **10**, 61–66.
- Chung, I., Han, J., Iwata, J. & Chai, Y. 2010. *Msx1* and *Dlx5* function synergistically to regulate frontal bone development. *Genesis* **48**, 645–655.

- Ciossek, T., Lerch, M. M. & Ullrich, A. 1995. Cloning, characterization, and differential expression of MDK2 and MDK5, two novel receptor tyrosine kinases of the eck/eph family. *Oncogene* **11**, 2085–2095.
- Copp, A. J., Greene, N. D. & Murdoch, J. N. 2003. The genetic basis of mammalian neurulation. *Nat. Rev. Genet.* **4**, 784–793.
- Depew, M. J., Liu, J. K., Long, J. E., Presley, R., Meneses, J. J., Pedersen, R. A. & Rubenstein, J. L. 1999. Dlx5 regulates regional development of the branchial arches and sensory capsules. *Development* **126**, 3831–3846.
- Depew, M. J., Simpson, C. A., Morasso, M. & Rubenstein, J. L. 2005. Reassessing the Dlx code: the genetic regulation of branchial arch skeletal pattern and development. *J. Anat.* **207**, 501–561.
- Frisen, J., Holmberg, J. & Barbacid, M. 1999. Ephrins and their eph receptors: multitasking directors of embryonic development. *EMBO J.* **18**, 5159–5165.
- Gilbert, S. F. 2003. *Developmental Biology*. Sinauer, USA.
- Han, M., Yang, X., Farrington, J. E. & Muneoka, K. 2003. Digit regeneration is regulated by Msx1 and BMP4 in fetal mice. *Development* **130**, 5123–5132.
- Han, J., Ishii, M., Bringas, P. Jr, Maas, R. L., Maxson, R. E. Jr & Chai, Y. 2007. Concerted action of Msx1 and Msx2 in regulating cranial neural crest cell differentiation during frontal bone development. *Mech. Dev.* **124**, 729–745.
- Holleville, N., Quilhac, A., Bontoux, M. & Monsoro-Burq, A. H. 2003. BMP signals regulate Dlx5 during early avian skull development. *Dev. Biol.* **257**, 177–189.
- Holmberg, J., Clarke, D. L. & Frisen, J. 2000. Regulation of repulsion versus adhesion by different splice forms of an eph receptor. *Nature* **408**, 203–206.
- Kim, H. J., Rice, D. P., Kettunen, P. J. & Thesleff, I. 1998. FGF-, BMP- and Shh-mediated signalling pathways in the regulation of cranial suture morphogenesis and calvarial bone development. *Development* **125**, 1241–1251.
- Kim, Y. J., Lee, M. H., Wozney, J. M., Cho, J. Y. & Ryoo, H. M. 2004. bone morphogenetic protein-2-induced alkaline phosphatase expression is stimulated by Dlx5 and repressed by Msx2. *J. Biol. Chem.* **279**, 50773–50780.
- Klein, R. 2009. bidirectional modulation of synaptic functions by eph/ephrin signaling. *Nat. Neurosci.* **12**, 15–20.
- Lallemant, Y., Nicola, M. A., Ramos, C., Bach, A., Clément, C. S. & Robert, B. 2005. Analysis of Msx1; Msx2 double mutants reveals multiple roles for msx genes in limb development. *Development* **132**, 3003–3014.
- Merlo, G. R., Zerega, B., Paleari, L., Trombino, S., Mantero, S. & Levi, G. 2000. multiple functions of Dlx genes. *Int. J. Dev. Biol.* **44**, 619–626.
- Muneoka, K., Wanek, N. & Bryant, S. V. 1986. Mouse embryos develop normally exo utero. *J. Exp. Zool.* **239**, 289–293.
- Newberry, E. P., Latifi, T. & Towler, D. A. 1998. Reciprocal regulation of osteocalcin transcription by the homeodomain proteins Msx2 and Dlx5. *Biochemistry* **37**, 16360–16368.
- Orvain, C., Matre, V. & Gabrielsen, O. S. 2008. The transcription factor c-Myb affects pre-mRNA splicing. *Biochem. Biophys. Res. Commun.* **372**, 309–313.
- Ramos, C. & Robert, B. 2005. Msh/Msx gene family in neural development. *Trends Genet.* **21**, 624–632.
- Robledo, R. F., Rajan, L., Li, X. & Lufkin, T. 2002. The Dlx5 and Dlx6 homeobox genes are essential for craniofacial, axial, and appendicular skeletal development. *Genes Dev.* **16**, 1089–1101.
- Satokata, I., Ma, L., Ohshima, H., Bei, M., Woo, I., Nishizawa, K., Maeda, T., Takano, Y., Uchiyama, M., Heaney, S., Peters, H., Tang, Z., Maxson, R. & Maas, R. 2000. Msx2 deficiency in mice causes pleiotropic defects in bone growth and ectodermal organ formation. *Nat. Genet.* **24**, 391–395.
- Satokata, I. & Maas, R. 1994. Msx1 deficient mice exhibit cleft palate and abnormalities of craniofacial and tooth development. *Nat. Genet.* **6**, 348–356.
- Shimeld, S. M., McKay, I. J. & Sharpe, P. T. 1996. The murine homeobox gene Msx-3 shows highly restricted expression in the developing neural tube. *Mech. Dev.* **55**, 201–210.
- Shirakabe, K., Terasawa, K., Miyama, K., Shibuya, H. & Nishida, E. 2001. Regulation of the activity of the transcription factor Runx2 by two homeobox proteins, Msx2 and Dlx5. *Genes Cells* **6**, 851–856.
- Timor-Tritsch, I. E., Greenebaum, E., Monteagudo, A. & Baxi, L. 1996. Exencephaly-anencephaly sequence: proof by ultrasound imaging and amniotic fluid cytology. *J. Matern. Fetal. Med.* **5**, 182–185.
- Valenzuela, D. M., Rojas, E., Griffiths, J. A., Compton, D. L., Gisser, M., Ip, N. Y., Goldfarb, M. & Yancopoulos, G. D. 1995. Identification of full-length and truncated forms of Ehk-3, a novel member of the eph receptor tyrosine kinase family. *Oncogene* **10**, 1573–1580.
- Wada, N. 2011. Spatiotemporal changes in cell adhesiveness during vertebrate limb morphogenesis. *Dev. Bio.* **240**(5), 969–978.
- Winograd, J., Reilly, M. P., Roe, R., Lutz, J., Laughner, E., Xu, X., Hu, L., Asakura, T., vander Kolk, C. & Strandberg, J. D. 1997. Perinatal lethality and multiple craniofacial malformations in MSX2 transgenic mice. *Hum. Mol. Genet.* **6**, 369–379.
- Zerucha, T., Stuhmer, T., Hatch, G., Park, B. K., Long, Q., Yu, G., Gambarotta, A., Schultz, J. R., Rubenstein, J. L. & Ecker, M. 2000. A highly conserved enhancer in the Dlx5/Dlx6 intergenic region is the site of cross-regulatory interactions between Dlx genes in the embryonic forebrain. *J. Neurosci.* **20**, 709–721.
- Zhang, H., Hu, G., Wang, H., Scivolino, P., Iler, N., Shen, M. M. & Abate-Shen, C. 1997. Heterodimerization of Msx and Dlx homeoproteins results in functional antagonism. *Mol. Cell. Biol.* **17**, 2920–2932.

Supporting Information

Additional Supporting Information may be found in the online version of this article:

Fig. S1. Gross morphology of WT, *Dlx5*^{−/−}, *Msx2*^{−/−}, and *Dlx5;Msx2*^{−/−} mouse embryos at E18.5. Note that, while cranial phenotypes vary depending on genotype, gross morphologies of embryos are not significantly altered from wildtype. Scale bar; 1 cm.